Characterization of ultrashallow junctions using frequency-dependent junction photovoltage and its lateral attenuation

V. N. Faifer[a] and M. I. Current
Frontier Semiconductor, San Jose, California 95112

D. K. Schroder
Department of Electrical Engineering, Arizona State University, Tempe, Arizona 85287-5706

(Received 17 May 2006; accepted 1 September 2006; published online 13 October 2006)

A contactless method for ultrashallow junction (USJ) characterization is described based on analysis of frequency-dependent junction photovoltages from illuminated and nonilluminated areas. Relevant equations for junction photovoltages are derived. It is shown that the measured leakage current in USJ formed in halo profiles is related to space-charge region recombination. © *2006 American Institute of Physics*. [DOI: 10.1063/1.2362596]

The requirement for source-drain extension junction depths <10 nm to control short-channel effects for <30 nm gates[1] has accelerated the development of methods for activation annealing, based on laser scans or "flash" light pulses, and junction monitoring metrology.

One-dimensional frequency-domain characterization of semiconductor parameters was discussed in Refs. 2–5. A rigorous two-dimensional, non-steady-state junction photovoltage (JPV) method was developed in Refs. 5 and 6 and implemented for measuring sheet resistance (R_S) and leakage current (I_0) in *p-n* junctions. In Refs. 5 and 6 good correlation of this noncontact technique and standard four-point probe (4PP) was demonstrated for deep (junction depth >50 nm) and low leakage current *p-n* junctions. In the case of ultra shallow junction (USJ) formed in heavily doped regions, e.g., halo or pocket doping, practically no correlation between JPV and 4PP methods was observed due to probe penetration and high leakage currents in *p-n* junctions.[6]

The present letter outlines an algorithm and theoretical background of a two-dimensional (2D) frequency-dependent JPV method for USJ characterization and describes the mechanisms responsible for the leakage current. The basis of the measurement is to use photoexcitation of carriers in the *p-n* junction and wafer substrate and to monitor, in a spatially resolved manner, the JPV signals inside and outside the illumination area. Two electrodes, a round transparent electrode (1) with diameter $2r_0$ at the center of the probe and a second round arc conducting electrode (2) subtending an angle β and coaxial with the first electrode some small distance away, are used for measurements of JPVs V_1 and V_2, respectively [Figs. 1(a) and 1(b)].[5]

Continuity and Poisson's equations were used to derive the two-dimensional JPV distribution, $v(x,y,t)$, and to obtain the voltages V_1 and V_2. Operating in the low-light excitation regime, where $v(x,y,t) \ll kT/q$, where k is Boltzmann's constant and T the Kelvin temperature, the junction photovoltage is proportional to the absorbed light flux and the variation of the surface space-charge region width W induced by illumination is small, allowing use of the one-dimensional Poisson equation at each point. By integration of the three-dimensional continuity equation over the vertical spatial coordinate z measured from the wafer surface $(0<z<x_j+W)$ and using a solution of the one-dimensional (1D) Poisson equation with assumption for substrate sheet resistance $R_{S\text{sub}} \ll R_S$, we obtain the 2D equation for the photovoltage distribution,

$$\frac{\partial^2 v}{\partial x^2} + \frac{\partial^2 v}{\partial y^2} = R_S C_{p\text{-}n} \frac{\partial v}{\partial t} + R_S G_{p\text{-}n} v - q\eta\Phi(1-R)R_S, \qquad (1)$$

where Φ is the light flux, η the efficiency, R the reflectivity, and R_S, $C_{p\text{-}n}$, and $G_{p\text{-}n}$ the *p-n* junction sheet resistance, capacitance, and conductance.

In the case of harmonic modulation of the light intensity, $\Phi(t)=\Phi_0(x,y)(1-\cos(2\pi ft))$, the junction photovoltage is

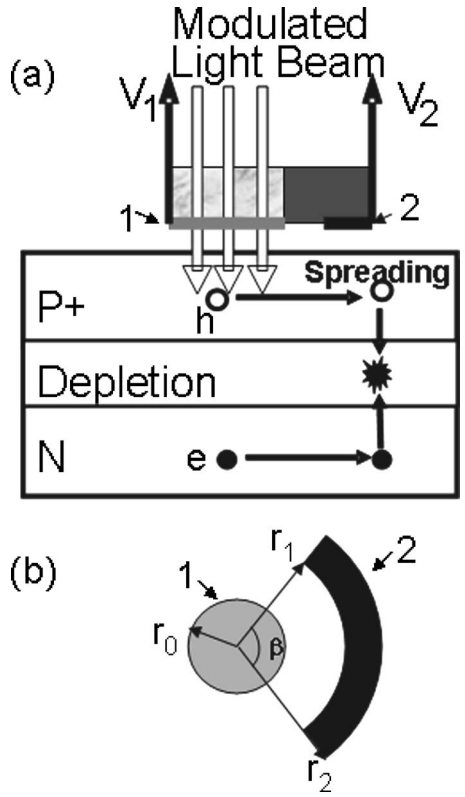

FIG. 1. (a) Photoexcitation and carrier drift with a modulated light source and two capacitor electrodes for monitoring the induced junction photovoltage in a spatially resolved manner; (b) electrode configuration.

[a]Electronic mail: fsm100@frontiersemi.com

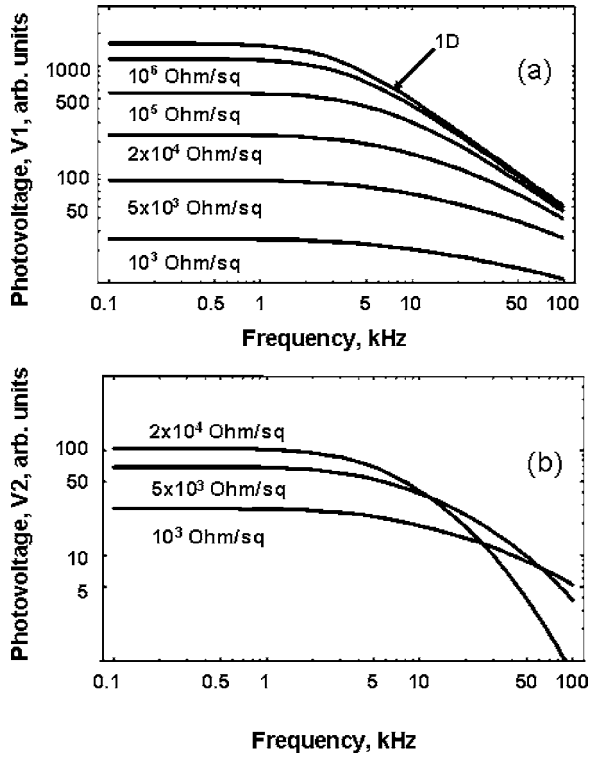

FIG. 2. JPVs (a) V_1 and (b) V_2 vs frequency calculated for 1D (infinite sheet resistance) and for 2D as a function of sheet resistance ($C_{p\text{-}n}=5\times10^{-9}$ F/cm^2, $I_0=2.6\times10^{-6}$ A/cm^2).

$v(x,y,t)=v_0(x,y)\cos(2\pi ft+\varphi(x,y))$. By solving Eq. (1) and taking the integral inside the illumination area, $r<r_0$, we determine the photovoltage signal from the circular transparent and conducting electrode as

$$V_1=\frac{q\eta(1-R)\Phi_0R_S}{k^2}\left[1-\frac{2}{kr_0}\frac{I_1(kr_0)K_1(kr_0)}{I_0(kr_0)K_1(kr_0)+I_1(kr_0)K_0(kr_0)}\right]. \quad (2)$$

By taking the integrals outside the illumination area, $r_0<r_1<r<r_2$, we get the photovoltage from the partially round arc conducting electrode subtending an angle β [Fig. 1(b)],

$$V_2=q\eta\frac{(1-R)\Phi_0\beta R_S}{\pi k^3r_0^2}\frac{I_1(kr_0)[r_1K_1(kr_1)-r_2K_1(kr_2)]}{I_0(kr_0)K_1(kr_0)+I_1(kr_0)K_0(kr_0)}, \quad (3)$$

where $I_0(z)$ and $I_1(z)$, and $K_0(z)$ and $K_1(z)$ are the modified Bessel functions and

$$k=\sqrt{R_SG_{p\text{-}n}+i2\pi fR_SC_{p\text{-}n}}. \quad (4)$$

The junction conductance $G_{p\text{-}n}$ and leakage current density I_0 are related by $G_{p\text{-}n}=I_0q/kT$. The theoretical frequency-dependent JPV V_1 for 1D (Ref. 4) and 2D algorithms and JPV V_2 for the 2D algorithm are shown in Fig. 2. For very high sheet resistance, $R_S\gg10^6$ Ω/sq, the 2D curves coincide with the 1D curve [Fig. 2(a)].[4] With decreasing sheet resistance, the 2D photovoltage decreases and the curves no longer have distinct corner frequencies like the 1D curve.[4]

By measuring the JPV at the two electrodes at different frequencies, combined with reference JPV measurements on a wafer with a deep p-n junction with known sheet resistance, the sheet resistance R_S conductance $G_{p\text{-}n}$, and capacitance of the p-n junction $C_{p\text{-}n}$ can be simultaneously determined using measured voltages V_1 and V_2 and Eqs. (2) and (3).

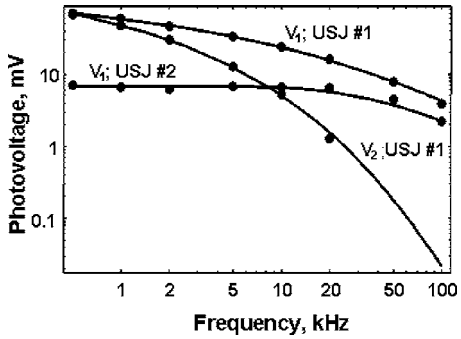

FIG. 3. JPVs V_1 and V_2 (points) and theoretical values (curves) vs light modulating frequency for USJ 1 (good p-n junction) and USJ 2 (leaky p-n junction).

The sheet resistance and leakage current of a laser annealed boron-doped $p^{++}n$ USJ formed in an As-doped ($N_D\approx10^{19}$ cm^{-3}) halo profile was measured. The experimental (points) and theoretical (curves) JPVs V_1 and V_2 versus frequency are shown in Fig. 3. The measured sheet resistance and leakage current in USJ 1 are $R_S=423$ Ω/sq and $I_0=10^{-6}$ A/cm^2. USJ 2 is very leaky with $I_0=2.5\times10^{-2}$ A/cm^2 and as a result, JPV signal V_2 being less than the noise voltage, $V_2<V_{\text{noise}}\approx0.3$ mV, the JPV V_2 is not shown in Fig. 3 and the sheet resistance of the second wafer was not determined.

This example demonstrates that rapid laser annealing can lead to high leakage current. Under illumination, the p-n junction is forward biased and the band-to-band tunneling effect is small since halo is not degenerate (i.e., Fermi level in halo is still within the band gap). The measured leakage current is determined by diffusion and recombination of excess carriers in the bulk, J_{diff}, recombination at the surface, J_S, and recombination in the space-charge region with trap assisted tunneling (TAT), J_W. In the case of uniform traps, an approximate expression is[4,7,8]

$$J_{\text{leak}}=J_{\text{diff}}+J_S+J_W\approx q\frac{n_i^2}{N_D}\sqrt{\frac{D_p}{\tau_p}}+qs_r\frac{n_i^2}{N_A}+\frac{qn_iW(1+\Gamma)}{\tau_g}, \quad (5)$$

where N_A and N_D are the acceptor and donor densities in the top layer of p-n junctions and in the halo profiles near the p-n junction, τ_g the generation lifetime in the p-n junction space-charge region, D_p and τ_p the hole diffusivity and lifetime in n-type halo profiles, W the space-charge region width, n_i the intrinsic carrier density, s_r the surface recombination velocity, and Γ the TAT factor.

For doping densities $N_A\approx10^{21}$ cm^{-3} and $N_D\approx5\times10^{18}$ cm^{-3} and maximum surface recombination velocity and diffusion velocity equal to the thermal velocity, $s_r=(D_p/\tau_p)^{0.5}=v_{\text{th}}\approx10^7$ cm/s, the bulk and surface recombination contribution $J_{\text{diff}}+J_s\approx10^{-10}$ A/cm^2 is very low compared to the measured leakage current and the space-charge region recombination current J_W dominates.

We compare the reverse-bias leakage current measured by the standard contact technique with this noncontact JPV

technique. The leakage current in heavily doped *p-n* junction under reverse bias includes two additional components: band-to-band tunneling current J_{tun} (Ref. 9) and thermionic emission current J_{them}.[10] In the case of heavily doped halo ($\sim 5\times 10^{18}$ cm^{-3}) and abrupt USJ, the band-to-band tunnel current density is $J_{tun}\approx 10^{-4}$ A/cm^2,[9] which sets the lower leakage current limit for the case of moderate trap densities. For this reason, the reverse-biased leakage current is sensitive to trap density in the space-charge region until $J_{tun} > J_W$. When the trap concentration is high and $J_{tun}<J_W$, the reverse-biased leakage current is proportional to the concentration of recombination centers in the space-charge region. We believe that the main contribution to J_W is related to insufficiently annealed end-of-range damage located in space-charge region which can result in high carrier trap concentrations. Leakage current measurements for heavily doped ($>10^{18}$ dopants/cm^3) substrates and halo profiles are consistent with carrier trap densities ranging from $N_{trap} \sim 10^{15}$ to $>10^{18}$ traps/cm^3 and trap capture cross section $\sigma=10^{-14}$ cm^2.[6]

In conclusion, we demonstrate a contactless two-dimensional frequency-dependent JPV method for USJ characterization. The key benefit of this method is the ability to obtain separate measurements of sheet resistance and leakage current, independent of junction depth, without the need for premeasurement surface preparation. The measured leakage current is directly linked to space-charge region recombination.

The authors acknowledge Ann Koo for support of this project and T. M. H. Wong and G. Mikhailov for discussions.

[1]See Table 69 in the Front End Process section of the ITRS05 (www.itrs.net).
[2]D. K. Schroder, J. E. Park, B. D. Choi, S. Kishino, and H. Yoshida, IEEE Trans. Electron Devices **47**, 1653 (2000).
[3]R. S. Nakhamson, Solid-State Electron. **18**, 617 (1975).
[4]J. E. Park, D. K. Schroder, S. E. Tan, B. D. Choi, M. Fletcher, A. Buczkowski, and F. Kirscht, J. Electrochem. Soc. **148**, G411 (2001).
[5]V. N. Faifer, M. I. Current, W. J. Walecki, V. V. Sushkov, G. Mikhailov, P. Van, T. Nguyen, T. M. H. Wong, J. Lu, S. H. Lau, and A. Koo, Mater. Res. Soc. Symp. Proc. **810**, 475 (2004).
[6]V. N. Faifer, M. I. Current, T. M. H. Wong, and V. V. Souchkov, J. Vac. Sci. Technol. B **24**, 414 (2006).
[7]G. A. M. Hurkx, D. B. M. Klassen, and M. P. Knuvers, IEEE Trans. Electron Devices **39**, 2090 (1992).
[8]J. E. Park, J. Shields, and D. K. Schroder, Solid-State Electron. **47**, 855 (2003).
[9]P. M. Solomon, D. J. Frank, J. Jopling, C. D'Emic, O. Dokumaci, P. Ronsheim, and W. E. Haensch, Tech. Dig. - Int. Electron Devices Meet. **2003**, 9.3.1.
[10]R. Lindsay, K. Henson, W. Vandervorst, K. Maex, B. J. Pawlak, R. Duffy, R. Surdeanu, P. Stolk, J. A. Kittl, S. Giangrandi, X. Pages, and K. van der Jeugd, J. Vac. Sci. Technol. B **22**, 306 (2004).